International Journal of Internet, Broadcasting and Communication Vol.16 No.1 330-338 (2024)
http://dx.doi.org/10.7236/IJIBC.2024.16.1.330

IJIBC 24-1-39

Ka-band Compact AESA Antenna Unit Design for Seeker

Bongmo Kang[1*], Ikjong Bae[2], Jaesub Han[3],
Youngwan. Kim[4], Jaehyun Shin[5], Jihan Joo[6], Seonghyun Ryu[7]

[1]Senior engineer, LIG NEX1 207, Mabuk-ro, Giheung-gu, Yongin-si, Gyeonggi-do Korea
bongmo.kang@lignex1.com

[2]Engineer, LIG NEX1 207, Mabuk-ro, Giheung-gu, Yongin-si, Gyeonggi-do, Korea
ikjong.bae@lignex1.com

[3]Chief engineer, LIG NEX1 207, Mabuk-ro, Giheung-gu, Yongin-si, Gyeonggi-do, Korea
jaesub.han@lignex1.com

[4]Chief engineer, LIG NEX1 207, Mabuk-ro, Giheung-gu, Yongin-si, Gyeonggi-do, Korea
youngwan.kim@lignex1.com

[5]Senior engineer, LIG NEX1 207, Mabuk-ro, Giheung-gu, Yongin-si, Gyeonggi-do, Korea
jaehyun.shin@lignex1.com

[6]Chief engineer, LIG NEX1 207, Mabuk-ro, Giheung-gu, Yongin-si, Gyeonggi-do, Korea
jihan.joo@lignex1.com

[7]Chief engineer, LIG NEX1 207, Mabuk-ro, Giheung-gu, Yongin-si, Gyeonggi-do, Korea
seonghyun.ryu@lignex1.com

**Correspondent Author: Bongmo Kang* (bongmo.kang@lignex1.com)*

Abstract

In this paper, a Ka-band high-output active phased array antenna device applicable to small radars and seekers was designed, and the improved performance was studied. The radiation device assembly consists of 1x8 arrangements, and the step flared notch antenna type. It shows low active reflection loss characteristics in broadband, and low loss characteristics by applying the air-strip feeding structure, and is designed to enable beam steering up to 45 degrees. The TRM(transmit receive module) output power is more than 2.0W per channel using GaN HPA in the transmitting path, and satisfies more than 25.0 dB gain and less than 6.0 dB noise figure in the receiving path. Accordingly, the Effective Isotropically Radiated Power(EIRP) of the antenna unit shows the performance of 0.00 dB or more and the receive gain-to-noise temperature ratio(G/T) of 0.00 dB/k or more. For demonstration, we have designed aforementioned planar array antenna which consists of 64 radiating elements having a size within 130 mm x 130 mm x 300 mm and weight of less than 4.9 kg..

Keywords: *AESA Antenna Unit, Compact, High-power, Ka-band, Light weight, Seeker, Step Flared Notch*

Manuscript Received: January. 22, 2024 / Revised: February. 2, 2024 / Accepted: February. 12, 2024
Corresponding Author: bongmo.kang@lignex1.com
Tel: +82-31-326-9409, Fax: +82-31-8026-7100
Senior engineer, LIG NEX1, 207, Mabuk-ro, Giheung-gu, Yongin-si, Gyeonggi-do, Korea

1. INTRODUCTION

Recently, active-phased array antennas are widely used in radar systems. The development of Beamformer IC has enabled a fast beam steering method for transmitting/receiving without the need for additional devices, especially in a compact size. Furthermore, advancements in GaN HPA(High Power Amplifier) technology have facilitated achieving high performance(efficiency and output) above the Ku band. We implemented an 8×8 active-phased array antenna unit that can be utilized in air-guided missiles and seekers by combining multiple TRMs, in which Beamformer IC and HPA technology are integrated. In this paper, we present the design of a low-noise stepped flare-type notch antenna with low-active reflection loss and a high power TRM with high receiving gain and a low noise figure. In addition, we detail the results of near-field tests for the antenna unit, including RF feed assembly, monopulse comparator assembly, drive assembly, switch assembly, and power/control components.

2. ANTENNA UNIT SYSTEM DEISNG AND PRODUCTION

Figure 1 shows the RF block diagram of the active-phased array antenna unit. The RF components include the drive assembly and the RF feed assembly. The drive assembly amplifies the transmitting signal from the external transceiver into a high-power output. The RF feed assembly uniformly distributes the amplified transmitted RF signal to the TRM or combines the amplified received RF signal and applies it to the monopulse comparator. The monopulse comparator receives the combined receiving signal from the RF feed assembly and separates them into sum, elevation difference, and azimuth difference channels through the combination of Rat-race circuit. The switch assembly amplifies the receiving signals with low noise and transmits them to the external transceiver [1]. Figure 2 shows the functional block diagram of the power/control component. The power/control components consist of the power supply assembly, control assembly, and motherboard. These components bypass or down convert DC power from external source for supplying power to active elements in TRM, drive assembly and switch assembly. In addition, it can generate TX/RX Enable signals and check BIT [2].

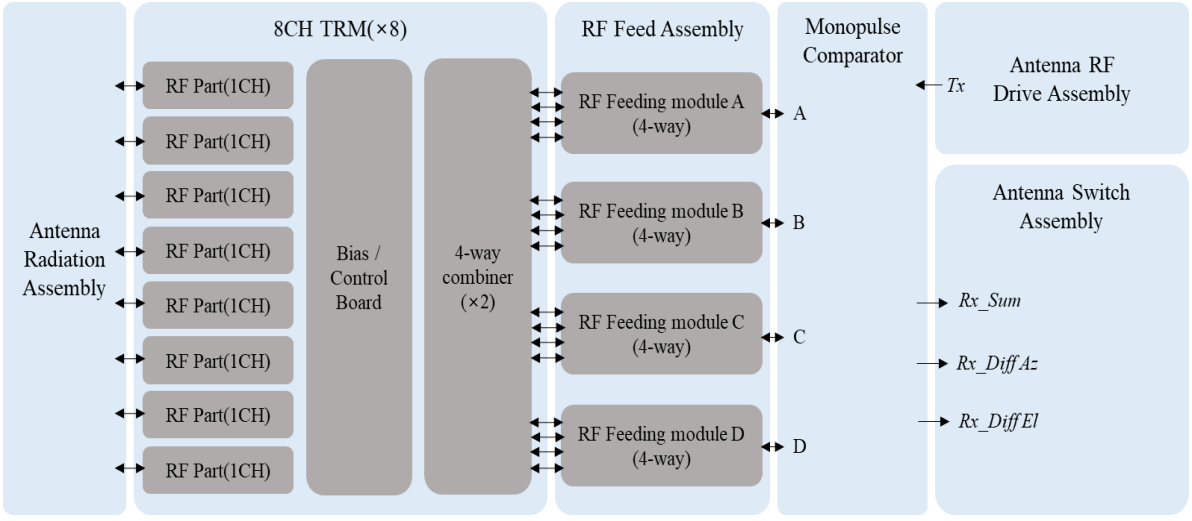

Figure 1. RF Block diagram of active phased array antenna unit

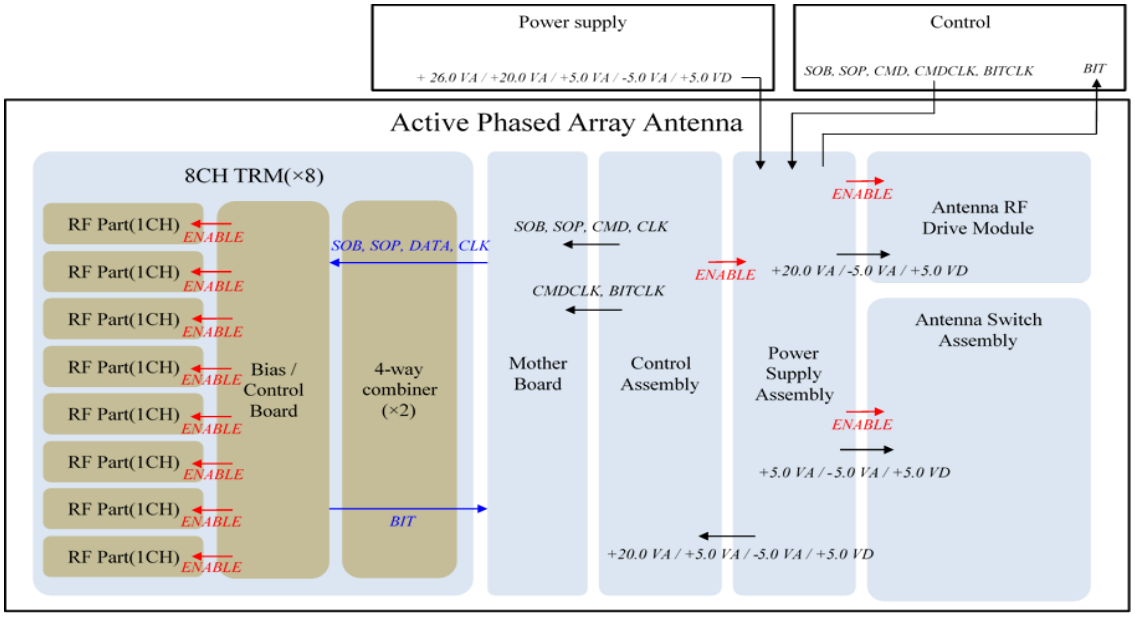

Figure 2. Power/Control Block diagram of active phased array antenna unit

3.1. DESIGN OF RADIATING ELEMENT ASSEMBLY

The radiating element assembly has an 8x8 array shape and consists of a total of 64 radiating elements as shown in figure 3. Additionally, the array spacing of the radiation element assembly was optimized to maximize gain while performing 45°(Theta in spherical coordinate system) beam steering. A single radiator was adopted as the Step Flare Notch(SFN) antenna that can implement broadband operation and low-profile. It is also advantageous for arrays as the amount of coupling with adjacent elements in less compared to the Vivaldi Notch Antenna [3].

Considering that the loss of transmission lines using dielectrics in the Ka-band is very large, the transmission lines were implemented with air striplines without dielectrics. When an active phased array antenna is operating, RF signals are supplied to each channel simultaneously. Therefore, the radiating element assembly must be designed taking into account active reflection coefficient of the radiating element assembly that can be calculated using the weight applied when forming each beam and the coupling coefficient between 64 radiating elements [4], [5].

Figure 4-(a) shows the active reflection coefficients in all beam steering range at each frequency, Figure 4-(b) is a graph showing the maximum and average values of active reflection coefficients at all frequencies.

After verifying it, the beam patterns of the radiation element assembly were verified by near-field measurement without TRM. The near-field measurement results were converted into far-field patterns after channel alignment using the individual measurement results of 64 channels, and the converted far field pattern can be seen in figure 4-(c).

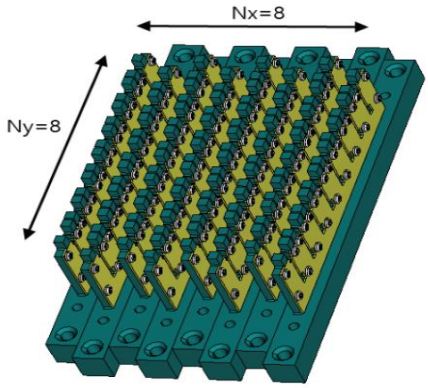

Figure 3. 8 by 8 radiating elements

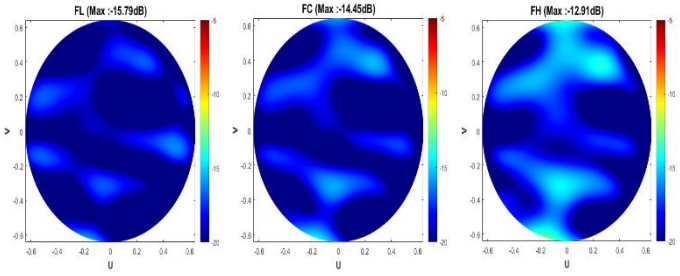

(a) Meas. results of reflection coefficient according to beam steering

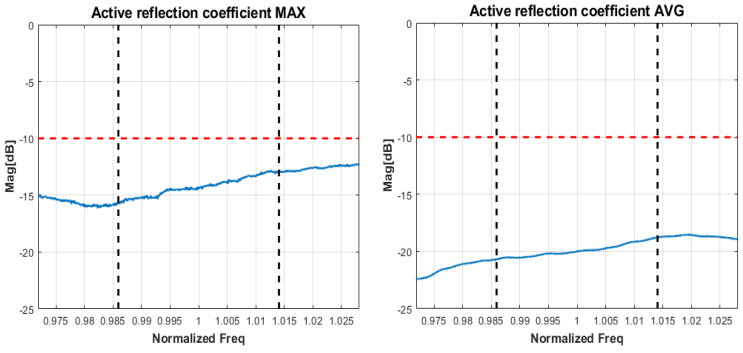

(b) Meas. results of reflection coefficient according to frequency

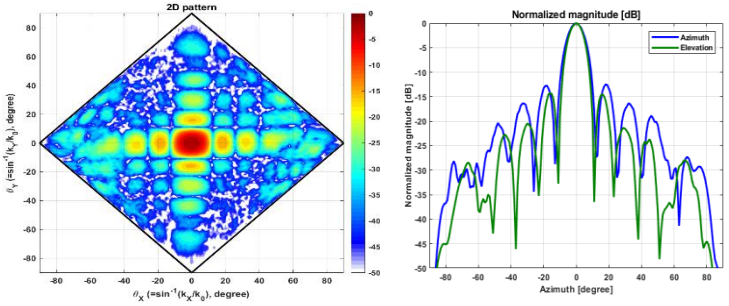

(c) Meas. results of pattern

Figure 4. Meas. result of antenna radiate element and assembly

3.2. DESIGN OF TRM

TRM performs various roles such as high-power amplification and low-noise amplification of RF signals, as well as separation of transmitting and receiving paths through SPDT and gain and phase shifting through Beamformer IC [6]. In this paper, a 64-channel active phased array antenna unit was designed by designing eight 1×8 channel brick-type TRMs, and heat dissipation fins were applied to the antenna unit housing for air-cooled heat dissipation. CPLD was used instead of FPGA to minimize specifications and power consumption. As shown in Figure 5, the TRM is divided into an RF part and a power control part. The specifications are W (54.0 mm) × D (140.0 mm) × H (4.8 mm), and the power consumption is less than 8.9 W.

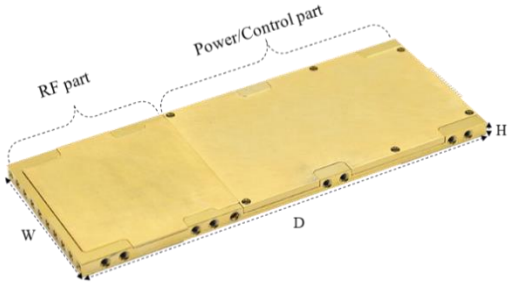

Figure 5. Designed TRM production shape

The measurement results and performance of the manufactured TRM are shown in Table 1 and Figure 6. The transmitting output at the target frequency is more than 2.1 W per channel, the receiving path gain is more than 27.6 dB, and the noise figure is less than 5.6 dB. In addition, gain and phase can be varied through the Beamformer IC in the TRM, but errors occur when varied. To check the changes in the beam pattern due to these errors, the beam pattern was analyzed when steering$(\theta = \phi = 0)$ in the Uniform, 25 dB Taylor receiving mode and compared to the ideal state without errors. The results are shown in Table 2.

Table 1. Measurement table of TRM

Component	Design value	Meas. result
Tx output power	$>$ 2.0 W	$>$ 2.1 W
Rx gain	$>$ 25.0 dB	$>$ 27.6 dB
Noise figure	$<$ 6.0 dB	$<$ 5.6 dB
Power consume	$<$ 10.0 W	$<$ 8.9 W
Weight	$<$ 150 g	$<$ 120 g

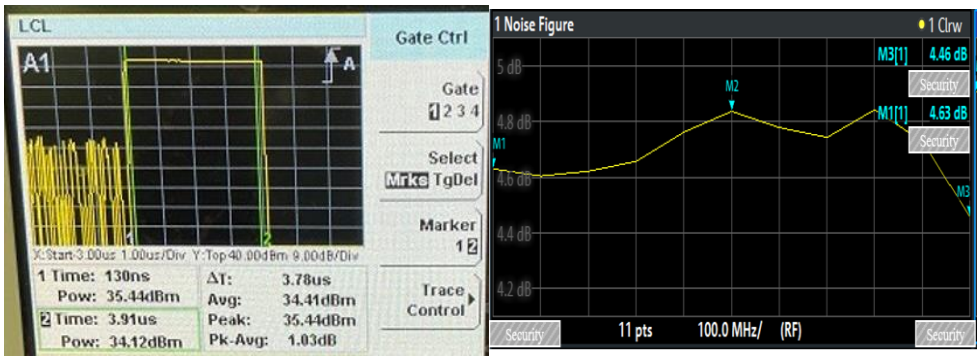

Figure 6. Mea. Results of TRM Tx output power and RX noise figure

Table 2. Beam pattern analysis result table of all TRM assembly channel magnitude, phase error

Component		2D SLL	Dir.	Beam pointing(θ, ϕ)
Tx / Rx Uniform	w/o error	-12.33	24.84	(0.058, 0.096)
	with error	-12.11	24.83	(0.057, 0.121)
Rx Taylor	w/o error	-22.87	23.53	(0.031, -0.033)
	with error	-22.37	23.52	(0.035, -0.038)

4. ACTIVE PHASED ARRAY ANTENNA UNIT TEST RESULTS

For verifying the presented active-phased array antenna unit, we have measured EIRP and G/T, and beam pattern by varying transmit/receive beam steering angle at near-field test site as shown in Figure 7. The mechanical alignment has been carried out before the near-field test and detailed measurement procedure at the near-field test site can be outlined as follows:

1) Measure Tx/Rx phase and Rx gain of each channel

2) Adjust gain and phase through TRM beamformer IC(electrical alignment)

3) Beam steering or changing to Taylor mode(Near-field test)

Table 3 shows the measured results of the side lobe level, HPBW and directivity by using with/without transmission electrical alignment.

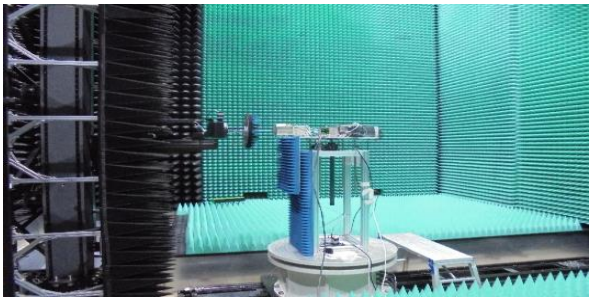

Figure 7. Picture of active phased array antenna unit at near-field measurement test

Table 3. Side lobe and directivity according to alignment of active phased array antenna unit

Component		2D SLL	HPBW.	Directivity
Rx	w/o align	-0.12	9.30	15.79
	with align	-10.90	11.36	23.40
Tx	w/o align	-2.36	13.88	18.03
	with align	-12.02	11.47	23.52

In this paper, an active-phased array antenna operating at the center frequency are well demonstrated. Transmit and receive(Uniform, 25 dB Taylor) tests were carried out, and it should be noted that the monopulse beam pattern results of receive test were verified through the difference pattern test of sum, azimuth difference and elevation difference as shown in Figure 8 and beam steering test [7] in Figure 9.

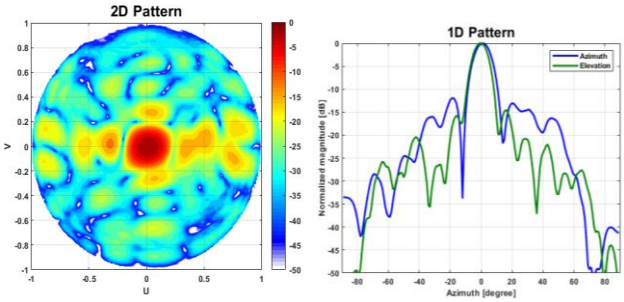

(a) Tx uniform weight 2D(left)/1D(right) pattern

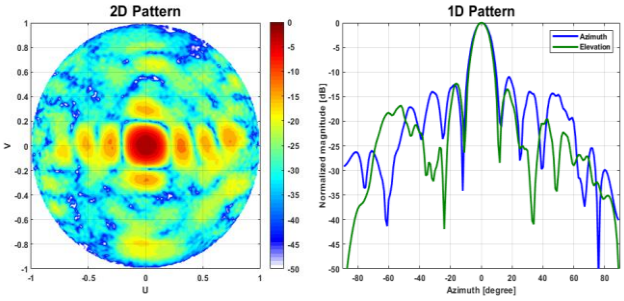

(b) Rx uniform weight 2D(left)/1D(right) pattern

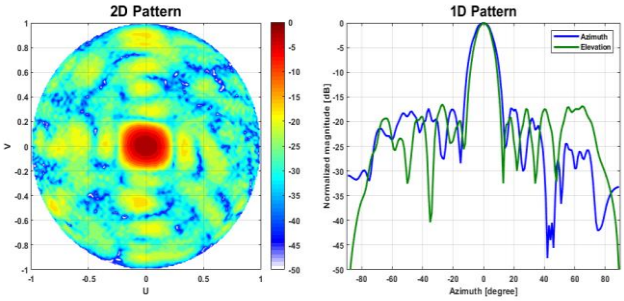

(c) Rx Taylor weight 2D(left)/1D(right) pattern

Figure 8. Tx/Rx beam pattern of active phased array antenna unit

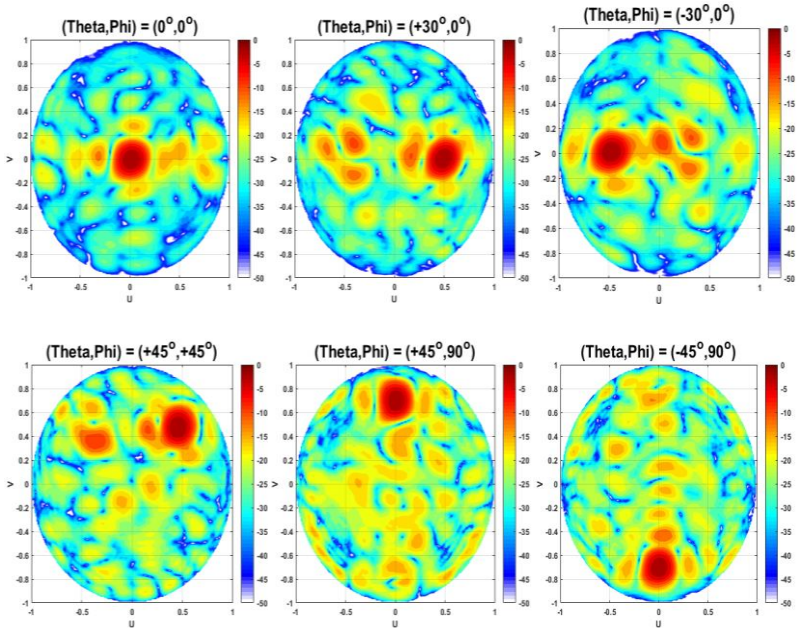

(a) Tx uniform beam steering pattern

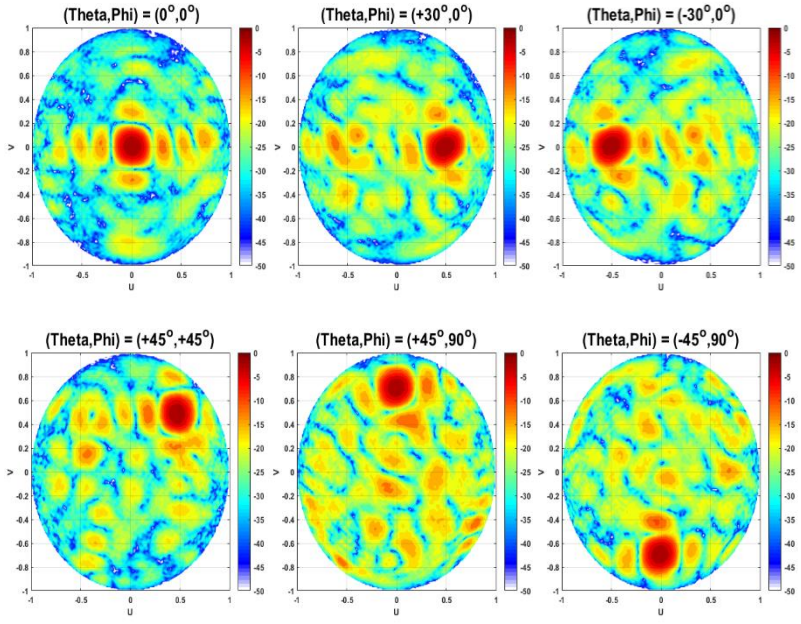

(b) Rx Taylor beam steering pattern

Figure 9. Tx/Rx beam steering pattern of active phased array antenna unit

5. CONCLUSION

This paper has presented a Ka-band high-power active-phased array antenna unit in compact size. Hence, it can be mounted on a small radar or seeker and Figure 8 shows the fabricated antenna. We have implemented

64 channels using 8 radiating element assembly and TRM composed of 8 channels. Figure 10 shows the overall shape of the antenna unit with its beam steering angle possible up to 00.0°. The measured maximum EIRP and the G/T are 00.0 dBmi and 00.0 dB/k (or higher), respectively. It is expected that improving maximum EIRP, G/T and wide-angle scanning can be possible by simply increasing the channel numbers.

Figure 10. Figure of active phased array antenna unit

REFERENCES

[1] J. S. Han, Y. W. Kim, J. G. Baek, J. P. Kim, "Design of Ka-band planar Active Phased Array Antenna," The Journal of Korean Society for Aeronautical & Space Sciences, vol. 47, no. 2, pp. 143-152, 2019. DOI: https://doi.org/10.5139/JKSAS.2019.47.2.143

[2] H. J. Jung, J. S. Han, et al., "Design and Fabrication of X-band Air-cooled, Compact, and Lightweight Active Eleectronically Scanned Array Antenna, " The Journal of Korean Institute of Electromagnetic Engineering and Science, vol. 34, no. 8, pp. 618-628, 2023. DOI https://doi.org/10.5515/KJKIEES.2023.34.8.618

[3] Y. W. Kim, J. G. Baek, H. E. Chae, J. H. Joo, "A Study on AESA Antenna Performance Advancement for Seeker," The Journal of The Institute of Internet, Broadcasting and Communication, vol. 23, no. 5, pp. 103-108, 2023. DOI: https://doi.org/10.7236/JIIBC.2023.23.5.103

[4] Y. W. Kim, J. B. Kwon, Y. D. Kang, J. K. Park, "Array Configuration Analysis of Ka-Band Phase Array Antenna," The Journal of The Institute of Internet, Broadcasting and Communication, vol. 19, no. 3, pp. 141-147, 2019. DOI: https://doi.org/10.7236/JIIBC.2019.19.3.141

[5] Y. W. Kim, H. D. Chae, S. H. An, J. H. Joo, "Radiator Design Method considering Wide-Angle Beam Steering Characteristics of AESA Radar," The Journal of The Institute of Internet, Broadcasting and Communication, vol. 22, no. 5, pp. 87-92, 2022. DOI: https://doi.org/10.7236/JIIBC.2022.22.5.87

[6] D. Y. Kim, et al "T/R Module Development for X-Band Phased-Array Radar," The Journal of Korean Institute of Electromagnetic Engineering and Science, vol. 20, no. 12, pp. 1243-1251, 2009. DOI: https://doi.org/10.5515/KJKIEES.2009.20.12.1243

[7] H. D. Chae, J. M. Joo, J. W. Yu, J. K. Park, "Subarray Structure Optimization Algorithm for Active Phased Array Antenna Using Recursive Element Exchanging Method," The Journal of Korean Institute of Electromagnetic Engineering and Science, vol. 27, no. 8, pp. 665-675, 2016. DOI: https://doi.org/10.5515/KJKIEES.2016.27.8.665